Experimental Research of FRP Composite Tube Confined Steel-reinforced Concrete Stub Columns Under Axial Compression

Ji Zhong WANG, Lu CHENG, Xin Pei WANG

Faculty of Instructure Engineering, Dalian University of Technology, Da'lian, Liaoning 116024, China

Abstract: A new column of FRP composite tube confined steel-reinforced concrete (FTCSRC) column was proposed. This paper elaborates on laboratorial and analytical studies on the behavior of FCTSRC columns subjected to axial compressive load. Eight circular FTCSRC stub columns and one circular steel tube confined concrete (STCC) stub column were tested to investigate the failure mode and axial compression performance of circular FTCRSC columns. Parametric analysis was implemented to inquire the influence of confinement material (CFRP-steel tube or CFRP-GFRP tube), internal steel and CFRP layers on the ultimate load capacity. CFRP-steel composite tube was composed of steel tube and CFRP layer which was wrapped outside the steel tube, while CFRP-GFRP composite tube was composite of GFRP tube and CFRP layer. The test results indicate that the confinement effect of CFRP-steel tube is greatly superior to CFRP-GFRP tube. The ductility performance of steel tube confined high-strength concrete column can be improved obviously by encasing steel in the core concrete. Furthermore, with the increase in the layers of FRP wraps, the axial load capacity increases greatly.

1 Introduction

Fiber-reinforced polymer (FRP) composites have been found wide practical applications in repair and restoration of concrete structures. In recent years, the application of FRP has increasingly in new construction as an efficient confinement material on account of its high strength-to-weight ratio and operability [1, 2]. It has been demonstrated in many studies that the load capacity and ductility of concrete structure can be improved by wrapping of FRP. However, the discrepancy between different types of FRP has a significant influence on the mechanical performance of structures [3]. GFRP has a good corrosion resistance with an inferior strength [4]. Hence, the use of combining the advantages of CFRP and GFRP with reinforced concrete has been widely explored as a new construction. FRP composite tube confined steel-reinforced concrete columns can resist the corrosion of steel efficiently [5, 6]. Confined tube can play a role of a shuttering which is beneficial to accelerate the construction process and reduce the construction cost.

The concept of FRP tube confined concrete was first proposed by Mirmiran A and Shahawy M [7, 8]. They conducted the parametric study, including concrete strength and the thickness of FRP tube, to inquire the influence of FRP. The results suggested that the load capacity of columns was enhanced remarkably. After that, there are a large number of studies in static properties of FRP confined concrete [9, 10]. The exploration about GFRP tube confined concrete has also made great process. While in the existing studies, the investigation on FRP composite confined high-strength concrete is few. The precious studies showed that the shear failure can be prevented by encasing steel in concrete.

This paper presents laboratorial and analytical studies on the compressive behavior of FTCSRC columns. The experimental program consists of 9 stub specimens to investigate the working mechanism and failure modes of composite columns. These test parameters considered include confinement material (CFRP-steel tube or CFRP-GFRP tube), internal steel and CFRP layers.

2 Experimental program

2.1. Materials and specimen preparation

In total, nine circular specimens, including eight FRP tube confined steel-reinforced concrete (FTCSRC) stub columns and one circular steel tube confined concrete (STCC) stub column, were designed and tested under axial compression. All the circular specimens had a diameter of 180mm (refer to the concrete core) and a height of 540mm. The type of inner steel is constant as

* Corresponding author: wangjz@dlut.edu.cn

No. 10a I-beam. The main tested parameters included the confinement material (FRP-steel tube or FRP-GFRP tube), the existence of internal steel and CFRP layers (0 (i.e., specimens without FRP sheet), 1, 2, 4 layers). The details of all the specimens are displayed in Table 1.

In the nomenclature of all specimens, for example, specimen "S-FTCSRC-1", S-FTCSRC represents CFRP-steel composite tube confined steel-reinforced concrete, 1 represents the CFRP layers. While G-FTCSRC represents CFRP-GFRP composite tube confined steel-reinforced concrete. STCC represents the steel tube confined concrete column.

Table 1 Specimen parameters and test results

Specimen	CFRP layers	N_e /KN	N_e / N_0	$\varepsilon_u/\mu\varepsilon$	$\varepsilon_u/\varepsilon_0$
STCC	0	2789	——	3.20	——
S-FTCSRC-0	0	3068	1	2.78	1
S-FTCSRC-1	1	3184	1.04	3.65	1.31
S-FTCSRC-2	2	3476	1.13	3.73	1.34
S-FTCSRC-4	4	4415	1.44	8.27	2.97
G-FTCSRC-0	0	2195	0.72	5.15	1.85
G-FTCSRC-1	1	2826	0.92	5.56	2
G-FTCSRC-2	2	3032	0.99	11.68	4.20
G-FTCSRC-4	4	3469	1.13	11.83	4.26

Standard tensile tests of flat coupons were conducted to identify the material properties of steel. The selection of steel type of inner steel was same as inner wrapping steel tube. The average values of the elastic modulus and yield stress were 212 GPa and 298 GPa. The circular steel tubes and GFRP tubes had the same inner diameter of 180mm and a thickness of 3mm. The steel tubes were manufactured by mild steel sheet and formed by modules. The GFRP tube in this paper was manufactured by Hebei Province. These GFRP tubes had a tensile strength of 240 MPa. In order to make sure that the confined tube does not take axial load directly, two small groves were carved at both edges of each specimen.

The used UT70-30 carbon fiber sheets were provided by Japan Toray Company. The CFRP sheets had a thickness of 0.167mm/ply (manufacturer data). The tensile strength and volume modulus of CFRP were provided by the manufacturer were 4216MPa and 252Gpa, respectively. JGN-T, a type of epoxy resin was adopted for gluing CFRPs together and adhering to the CFRP to the steel tube or GFRP tube by a hand-up method. To ensure the entire confinement, the finishing end of a sheet overlapped the starting end by 200mm.

The design level of concrete was C80 which belongs to high-strength concrete, and a group of cubes were cast and cured in similar conditions to the related specimens. Prior to casting, a steel plate with thickness of 20mm was welded to the steel tube at one end. Then these specimens were placed upright to air-der until testing. Fig. 1 shows the concrete configuration of specimens.

2.2. Test setup and instrumentation

The specimen tests were conducted at Dalian university of Technology using a 10000 kN capacity universal testing machine. The load was added on the specimen directly by hydraulic jack and monitored. Axial deformation of the column was measured by using four linear variable displacement transducers (LVDT) which were kept at top of the jack. Sixteen strain gauges, including twelve in the longitudinal direction and another four in the transverse direction, stuck on the external surface of each specimen at top, mid-height and bottom. The loading process can be divided into three phases. The loading was applied with load control at 1.5kN per second at the initial stage. After that, displacement control was used at approximately 0.3mm per second until specimen failure. All test data, including strains, displacements and loads, were completely recorded. The load at which the CFRP starts rupturing and the failure symptom of specimens were also marked for every specimen. Fig. 2 shows the loading arrangement.

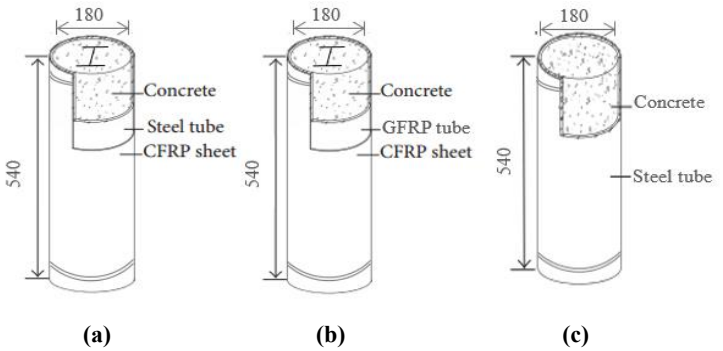

(a) **(b)** **(c)**

Fig. 1 Concrete configuration of tested columns
(a) S-FTCSRC; (b) G-FTCSRC; (c) STCC

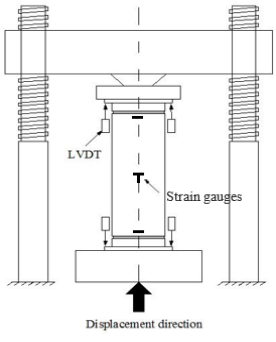

Fig.2 load system

2.3. Experimental Results and Failure modes

For the two specimens with steel tube (i.e., specimens S-FCTSRC-0 and STCC), there is not obvious phenomenon in the appearance during the initial loading process. When the load attains about 85% of the maximum load (Ne), the remarkable buckling can be observed at the mid-height cross-section. For the G-FTCSRC-0 specimen, the change in the outward appearance is also invisible until to the ultimate load. The white hairline crack can be observed and an abrupt fracture occurs with a big noise.

In the case of CFRP strengthened specimens, as shown in Fig.3, snapping sound of the oxide layers peeling can be heard as axial load increase. For CFRP-steel tube, the rupture of fibers occurred after steel tube yielded. The wrapping CFRP sheet was activated by the significant lateral deformation. However, the CFRP sheets of G-FCTSRC stub columns rupture randomly accompanied with the fracture of GFRP tube. The reason for this different failure modes about two different confinement material could be that GFRP is more brittle than steel [11].

Fig.3 also shows failure modes of the concrete after cutting off the composite specimens. It can be observed that CFRP sheets provide effectively restraint against the lateral deformation of core concrete. Similar shear failure was observed in all columns tested. It is interesting that the cracks on the surface of the concrete was tinier in S-FTCSRC-0 than STCC because of the existence of inserted steel shape. It can be explained that the inserted steel shape restricted the development of the slip in core concrete within half side of the cross-section.

Fig. 3 Failure modes of specimens

3 Parametric study

3.1. The effect of confinement material

In the following analysis, the axial load-displacement relationship is used to investigate the influence of different parameters. Fig.5 shows the influence of confinement material on the specimens under different CFRP layers. The relative values about ultimate load capacity and axial deformation are also summarized in Table.1. Axial load capacities of G-FCTSRC columns is lower than S-FCTSRC-0 except at the 4 CFRP layers, which means that ultimate load of S-FCTSRC columns is obviously higher than G-FCTSRC. In the contrary, the axial deformation of G-FCTSRC is superior to S-FCTSRC columns at peak load. The relative values about $\varepsilon_u/\varepsilon_0$ of S-FTCSRC-4, G-FTCSRC-4 were 2.97 and 4.26, respectively.

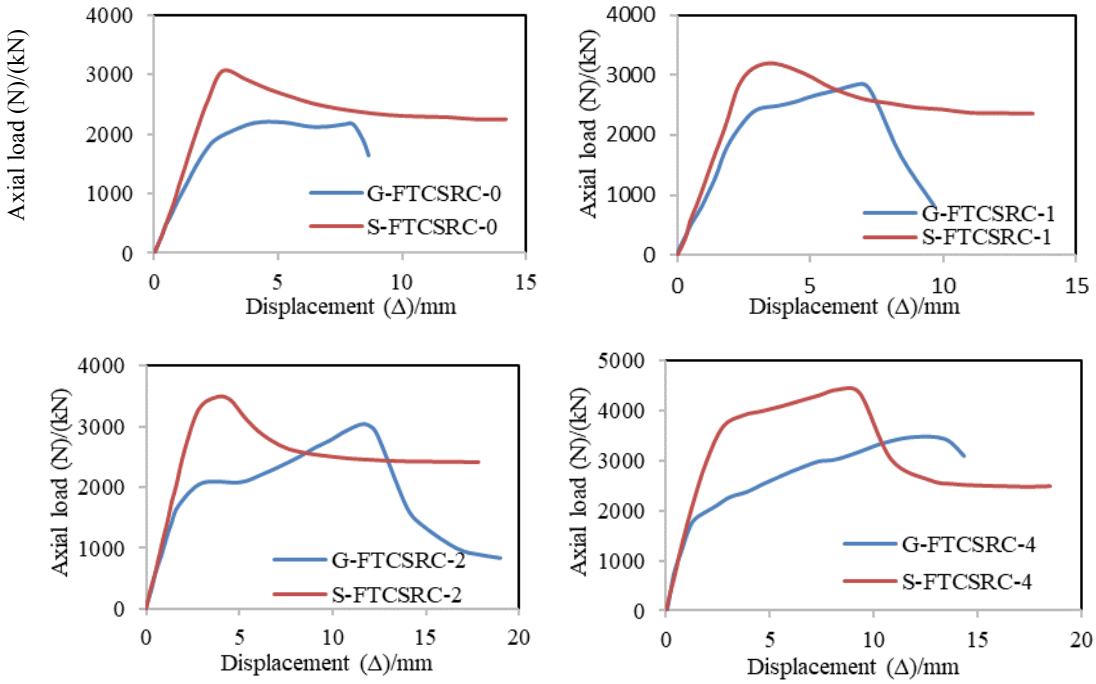

Fig.5 load-displacement curves about different confinement material

3.2. The effect of internal steel

Fig.6 shows the impact of inner steel on the specimens whose parameters are the same except an internal steel shape. It can be demonstrated that encasing internal steel has a small increment in elastic module and load capacity. After the peak load, the downward trend of S-FTCSRC-0 is gentler than STCC. For S-FTCSRC-0, the load remains a stable value approximately about 2300 kN in the later period, which is higher than STCC about 1700 kN correspondingly.

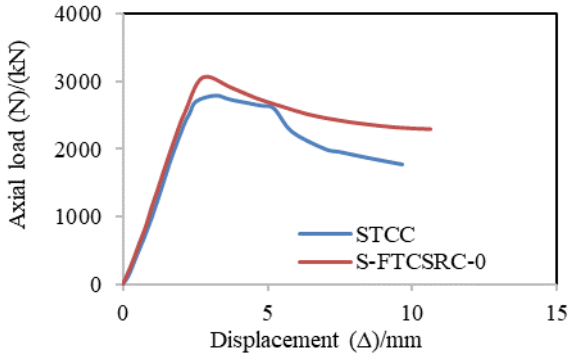

Fig.6 load-displacement curves about internal steel

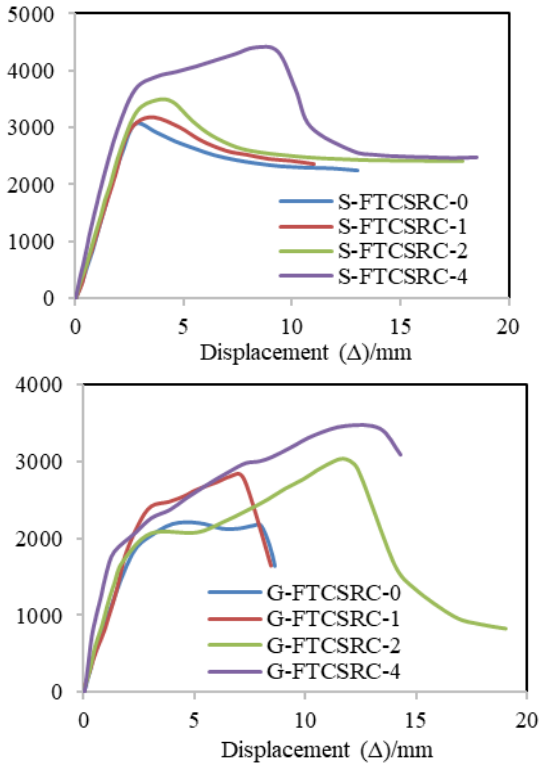

Fig.7 load-displacement curves about different CFRP layers

3.2. The effect of CFRP layers

The tested axial load versus displacement curves of the specimens are shown in Fig.7. It demonstrates that the specimens are under elasticity in the initial stage because the curves are straight. As the load increases, the CFRP sheets were gradually activated by remarkable convex deformation of concrete. The amount of the axial load and the axial displacement where maximum load capacity are increased as the number of CFRP sheet layers increased. The use of a thicker CFRP sheets leads to a second linear ascending portion. In particular, the G-FCTSRC column has a larger and more distinct slope for the second portion of the curves because CFRP sheets restrain the GFRP tube more valid with its lower strength.

4 Conclusion

(1) The buckling of core concrete was well confined in F-CTSRC columns, leading to a very strength and ductile response under axial compression.

(2) The axial load capacity of S-FTCSRCs is higher than G-FCTSRCs, but the ductility of the S-FCTSRCs is inferior to the G-FTCSRCs.

(3) The existence of internal steel has an obvious influence in the failure modes of STCCs, in which the shear failure could be deterred.

(4) The load capacity and axial deformation of FTCSRC columns was enhanced as the number of CFRP sheet layers increased, however, the induction can be concluded that G-FTCSRC columns perform a better performance both in strength and ductility when the wrapping CFRP sheets are thick enough.

References

1. Saadatmanesh H. Fiber composites for new and existing structures[J]. Aci Structural Journal, 1994, 91(3): 346-354.
2. Tanwongsval S, Maalej M, Paramasivam P. Strengthening of RC wall-like columns with FRP under sustained loading[J]. Materials & Structures, 2003, 36(5): 282-290.
3. Lau K T, Zhou L M. Mechanical performance of composite-strengthened concrete structures[J]. Composites Part B Engineering, 2001, 32(1): 21-31.
4. Sheikh S A, Jaffry S A D, Cui C. Investigation of glass-fibre-reinforced-polymer shells as formwork and. [J]. Canadian Journal of Civil Engineering, 2007, 34(3): 389-402.
5. Xiao J, Huang Y. On the seismic behavior and damage assessment of recycled aggregate concrete filled GFRP tube column[J]. China Civil Engineering Journal, 2012, 45(11): 112-120.
6. Mirmiran A, Shahawy M. A new concrete-filled hollow FRP composite column[J]. Composites Part B Engineering, 1996, 27(3–4): 263-268.
7. Mirmiran A, Shahawy M. Behavior of concrete columns confined by fiber composites[J]. Journal of Structural Engineering, 1997, 123(5): 583-590.
8. Zhu Z, Ahmad I, Mirmiran A. Effect of Column Parameters on Axial Compression Behavior of Concrete-Filled FRP Tubes[J]. Advances in Structural Engineering, 2005, 8(4): 443-450.
9. Ozbakkaloglu T, Saatcioglu M. Seismic Behavior of High-Strength Concrete Columns Confined by Fiber-Reinforced Polymer Tubes[J]. Journal of Composites for Construction, 2006, 10(6): 538-549.
10. Wang L G, Chen B L. Steel Reinforced Concrete-Filled Glass Fiber Reinforced Polymer or Steel Tubular Structures[M]. Liaoning Scientific & Technical Publishers, Shenyang, 2013.
11. Wang L G, Qin G P, Zhou L. Experimental research of gfrp tube columns filled with steel-reinforced high-strength concrete subjected to axial loading[J]. Engineering Mechanics, 2009.